(NASA-TM-86119) OBSERVATIONS OF THE EARTH'S MAGNETIC FIELD FROM THE SPACE STATION: MEASUREMENT AT HIGH AND EXTREMELY LOW ALTITUDE USING SPACE STATION-CONTROLLED FREE-FLYERS (NASA) 52 p HC A04/MF A01 CSCL G3/46

N84-26183

Unclas
19473

NASA

Technical Memorandum 86119

OBSERVATIONS OF THE EARTH'S MAGNETIC FIELD FROM THE SPACE STATION: MEASUREMENT AT HIGH AND EXTREMELY LOW ALTITUDE USING SPACE STATION-CONTROLLED FREE-FLYERS

William J. Webster, Jr.
Geophysics Branch
Goddard Space Flight Center
Greenbelt, MD 20771

James J. Frawley
Science Systems and Applications, Inc.
Seabrook MD 20706

Michael Stefanik
Science Systems and Applications, Inc.
Seabrook, MD 20706

MAY 1984

National Aeronautics and
Space Administration

Goddard Space Flight Center
Greenbelt, Maryland 20771

OBSERVATIONS OF THE EARTH'S MAGNETIC FIELD FROM THE SPACE STATION: MEASUREMENT AT HIGH AND EXTREMELY LOW ALTITUDE USING SPACE STATION-CONTROLLED FREE-FLYERS

William J. Webster, Jr.
Geophysics Branch
Goddard Space Flight Center
Greenbelt, MD 20771

James J. Frawley
Science Systems and Applications, Inc.
Seabrook, MD 20706

Michael Stefanik
Science Systems and Applications, Inc.
Seabrook, MD 20706

OBSERVATIONS OF THE EARTH'S MAGNETIC FIELD FROM THE SPACE STATION: MEASUREMENT AT HIGH AND EXTREMELY LOW ALTITUDE USING SPACE STATION-CONTROLLED FREE-FLYERS

Executive Summary

Introduction

In this study, we are concerned with the application of the space station's capabilities in studying the sources of the observed magnetic field which are identified with the earth i.e., the core and crust. Two basic systems will be required to pursue these objectives.

To study the core source, absolute observations of at least the scalar (vector preferred) field are required at intervals over an extremely long period (tens of years). The data rate is sufficiently low that processing could be done on-board the station.

To study the crustal sources at high strength and to observe the effect of ionospheric currents close to the source, observations are needed at lower altitude than is possible for a space station. To satisfy this requirement, a free-flyer capable of operation near 100 km is required.

Results

a. High Altitude

Experience with Magsat has shown that two days worth of magnetically quiet data taken in a polar orbit suffices to produce a high quality model of the main field. Observations of comparable quality spaced over a long (10 year) period would determine the secular variation to a far greater accuracy that has ever been possible. In particular, it should be possible to establish whether the variation is linear or more complex. Two major problems were addressed in considering these measurements in a space station environment:

1. How large an influence would a non-polar orbit have on the determination of the main field and how well must that orbit be known?

A global magnetic field array was generated. This array, calculated from the best Magsat model, was used to confirm the theoretical prediction that the accuracy of recovering the first four components of the main field scales roughly as the square of the orbital inclination. The results indicate that inclinations above 33^{o} give an acceptable model quality while 50^{o} or greater gives models equivalent to the Magsat results. A repeat of the orbital error analysis made for Magsat was made using the Magsat (rather than POGO) field model. 100 m along track, 60 m cross track and 60 m radial accuracies will produce measurement errors comparable to Magsat.

2. How far must the space station and the magnetometer be separated? In general, magnetometers tend to be limited not by instrumentally generated noise but rather by environmental noise. Environmental noise often cannot be controlled and as a result, the magnetometer must be displaced from its spacecraft. In the case of Magsat, stringent measures were required to keep the boom length as small as 6 m. In the case of the space station, strict magnetic suppression can probably not be undertaken. As a result, the magnetometer will have to be a considerable distance from the station. Clearly, it is not possible to specify an exact distance until the space station is designed in detail. However, the magnetic moment provides a means of estimating the minimum required separation. Since the instruments are capable of 0.5 nT sensitivity, we specify a distance required to attenuate the noise to 0.5 nT. For an object with the magnetic moment of the space shuttle orbiter, the external fields due to the orbiter require a separation of at least 0.8 km. The scaling with distance is roughly proportional to distance cubed.

b. Low Altitude

The contribution to the total measured field at 600 km due to the crustal component is about 20 nT out of 5×10^4 nT while the currents can be responsible for about 10^3 nT out of the 5×10^4 nT. Clearly, measurement of especially the crustal component is best conducted as close to the source as is practical. Accordingly, conventional satellite observations for crustal field studies have been considered at an altitude of 160 km. Operation at such low altitudes or at lower altitudes is dependent on such considerations as the required specific impulse of the maneuver engine, consequences of aerodynamic heating and the location and altitude of the various components of the earth's current system.

In-situ measurements by the Atmospheric Explorer satellites at altitudes as low as 90 km permit a calculation of the level of disturbing field due to the formation of a plasma wake and its associated boundary shocks. Similar phenomena have been observed on the shuttle at much higher altitude. The field is calculated from the charge density and apparent velocity measured by the AE (and other) experiments. Observations at altitudes less than 100 km are probably not possible.

The improvement in resolution to be anticipated by lowering the altitude of observation has been demonstrated by the comparison of simultaneous POGO 4 and Magsat passes over the same area. In order to quantify this effect, we have computed the resulting field from long (20^o of latitude), thin (0.5^o of longitude) bodies at various altitudes. The increase in field strength and resolution at 100 km results in a 50% improvement in resolution and a factor of about 4 improvement in sensitivity over Magsat.

Introduction

Observations of the earth's magnetic field from space have been conducted since the beginning of the space age (Sputnik 3, 1958). With the recently completed Magsat mission, these observations have reached a level of sophistication which has permitted scientific investigation of the earth's core, crust and magnetosphere in detail.

The Magsat observations have provided high quality models of the main (core component) field and crustal fields. Together with observations of the magnetosphere at higher altitudes provided by various satellites, a complete description of the earth's field is available for the epoch of the Magsat observations.

Because of the known time variability of the high altitude magnetosphere component and the core component, observations over an extended period of time would serve to define the time scale of variation. In view of recent evidence of short time-scale variations of the core component, the time scale of the observations may be critical in defining the core circulation pattern which is presumably responsible for the changes. An improvement on the crustal data is possible by observing at a lower altitude than Magsat and/or from a non-polar orbit. In this study, we are concerned with the core and crustal field components and how these field components might best be measured in the space station era.

The advent of a permanent space station in the 1990s promises to provide a means for conducting long duration experiments totally unlike previous space operations. Although Skylab has been suggested as a model, external operations by the crew seem much more likely with the space station. It is likely that most maintenance and manual calibration tasks will either be performed on or near the station or by personnel or teleoperators dispatched from the station. These factors will likely change the way in which measurements are made in space to a more laboratory like setting.

Although the measuring systems, as we shall see, can only be loosely tied (in a physical sense) to the station, the availability of the station's resources makes possible a complexity of operation which would be very costly to implement in other ways.

Study Philosophy

In this work, we are concerned with the core and crustal component of the earth's field. We will define the characteristics of the measurement systems required to derive these two components with a quality equal to or better than was obtained with Magsat. With these results, we will then assess the impact of the availability of the space station on the scientific objectives of the measurements. We will then consider the level of effort required from the station crew to support the scientific objectives.

For each of the two kinds of measurements, we will first examine the mission requirements to produce data of the required quality. We will use the Magsat results as a standard of comparison and show how the expected results compare for different orbital parameters and altitude regimes. We will then establish the instrumental requirements to perform the measurements.

We will divide the kinds of measurements into observing altitude regimes. We will define as high altitude those observations which would be made at altitudes equal to or greater than 200 km. Although the crustal field would be discernable in these data, such measurements would be most useful in defining the core component and its temporal and spatial variations. Low altitude observations will be defined to be at less than 200 km.

High Altitude Observations

In considering the high altitude case, we will adopt the following ground rules:

1. We will assume that the station will operate in a non-polar orbit at an altitude of 200 km. We will also assume that the station is accessible by KSC launched shuttles.

2. We will assume that any instrument package must be accessible to or be directly controlled by the station. This implies that, although the package could be in a different orbit, it must be in a similar orbit.

High altitude observations would be directed toward measurements of the core component of the earth's field. Although the study altitude is lower than the bulk of the Magsat observations, we will restrict our consideration of the crustal and magnetospheric fields to the lower altitude observations. It is clear, however, that an improved map of the crustal field is possible from observation at 200 km altitude even though the core field is the prime interest.

In studying the core component, we are interested in two factors:

1. We wish to define the spatial variation of the core component at a given epoch to at least the accuracy of the Magsat results.

2. Since the core field varies with time, we need to make observations at intervals. It is important to note that the time scale over which the core field shows significant variation is not known.

We can assess the requirements for the high altitude by answering the following questions.

1. How does the inclination of the orbit influence the ability to measure the core field and its time variation?

2. How accurately must the orbit be known?

3. How far must the instrument package be separated from the station to minimize the influence of the station's magnetic moment?

4. What instrument complement will be best for the defined measurements?

We address the instrument complement first since this impacts the other considerations. Up until the time of the Magsat mission, the best available global data set was provided by the three Orbiting Geophysical Observatory (OGO) satellites. These satellites carried, among other experiments, a high accuracy scalar magnetometer which observed the scalar field with a roughly 6 nT accuracy. These satellites provided the highest quality models of the core field until Magsat.

It should be noted that the OGO observations were made with a scalar magnetometer. The conventional analysis of these data involves the fitting of a two-dimensional spherical harmonic series to the data. From this expansion, the values of various current moments can be derived. Since the scalar data only contains indirect information on field direction, the estimation process can produce harmonic coefficients whose true error is much larger than the error of the whole representation (Backus, 1970). An analysis of the OGO situation by Stern and Bredekamp (1975) shows that the Backus effect has a profound influence on especially the high order coefficients.

Because of this effect, the field models for Magsat used vector measurements. A scalar magnetometer was flown on Magsat but, the scalar magnetometer was used strictly to calibrate the vector instrument. Stern, Langel and Mead (1980), using the Magsat vector measurements, showed that, for identical observation grids, the use of scalar data (derived directly from the vector data) leads to large differences between the scalar and vector model. This work clearly confirms the theory and demonstrates that a vector magnetometer is the preferred instrument for observing the core field.

At the time of the Magsat mission, magnetometer technology was not sufficient to provide an absolute vector magnetometer at low cost. As a result, the Magsat instrument complement consisted of an absolute scalar magnetometer (Farthing, 1980) and a high-stability, flux gate vector magnetometer (Acuna, 1980). The scalar instrument was used to provide an absolute calibration for the vector magnetometer. This permitted a continuous update of the vector calibration throughout the observations.

The modeling schema adopted for the Magsat applies directly to the kind of observations we are considering here. Except in regions where the influence of magnetospheric and ionospheric currents is expected, the vector data is used. In the disturbed regions (latitude > 50^o and over the equatorial current system), Langel (1974) has shown that the scalar field is little disturbed and, therefore, suitable for inclusion in modeling. The individual vector components can, thus, be used to decide when the scalar field must be used. If the instrument technology has not advanced to the state where a low-cost absolute vector magnetometer is possible, a core-field-directed mission would require both kinds of magnetometers.

We next consider the influence of orbit parameters on the core field measurements. Clearly, a determination of the various field moments depends on measurements of the field geometry. The determination of geometry of the field obviously depends on the extent to which the measuring orbit covers the regions where the flux density is changing most quickly with geographic coordinates. Accordingly, the best determination of the core field moments is made from an orbit which passes over the magnetic poles as was the case for Magsat.

We have assumed that the space station is accessible from KSC. Thus, in addition to assuming that the mean orbit altitude is 200 km, we have assumed that the orbit inclination is less than 60°. This orbit, of course, does not pass over the magnetic poles. It is now necessary to derive the performance to be expected for orbital inclinations less than 60°. To summarize, in what follows, we assume:

1. 200 km circular orbit.
2. Orbital inclination less than 60°.
3. Scalar magnetometer with instrument noise of 0.5 nT.
4. No significant contribution from the current system.

We will first begin with the field moments for the case of instrument noise only. Next, we will add 6 nT rms environmental noise. Finally, we will consider a simultaneous solution for the field moments and the secular variation over a 4 year period.

The basis of this analysis was a grid of scalar field values calculated with the MGST-481#2 field model. The grid spacing was 5° in latitude and longitude and covered that latitude band between ±60°. The grid was calculated both for epoch 1980.0 with no time terms and for the same epoch with time terms corresponding to four years of temporal variation.

The fitting of the spherical harmonic series to the data was performed with the same program used to prepare the Magsat model (Estes, 1983). This program is a least-squares estimator which works on non-linear data and performs the solution iteratively. In this study, we also made use of the program's ability to introduce random noise into each measurement.

In the estimations, we have assumed that each cell having an absolute value of latitude less than or equal to the inclination of the measuring orbit has been sampled. This is equivalent to assuming that the data covers at least three days worth of orbits (Webster, 1983). A previous study (Webster, 1983) has shown that, although it is not likely that three consecutive days suitable for field modeling will occur especially during the peak of the solar cycle, it is likely that three suitable days will be found in any ten day interval.

In each of the cases which follow, we first fit the entire grid and use this as the standard of comparison for the fits for other inclinations. It should be noted that the result of the full-grid fit is a priori 9 times poorer than the Magsat model itself since we are dealing with scalar rather than vector data. Also, our fits will show the effect of the Backus phenomenon. This will be especially evident for terms with n=m. We have also observed that the fit distributes the bulk of the spectral power into the n=2 and 3 coefficients. Residual spectral power not accounted for by the low order coefficients tended to be distributed among the high order coefficients in a noise-like manner. This was especially true for inclinations 30° or less. Accordingly, although we fit a full 12x12 set of coefficients (plus time terms where appropriate) we will tabulate only the second and third degree deviations from the 60° case.

In Table 1, we give the results for the noise free case. Note that the rms error of the representation drops very quickly until it levels out between 30° and 45° inclination. In Figure 1, we plot the rms error for all the cases computed. It is clear that up until 33°, a small change in inclination makes a big improvement in the results. Above 33°, a much larger change in inclination is required for an equivalent improvement. In Figure 2, we show

TABLE 1

DEVIATIONS OF INDIVIDUAL MOMENTS FROM FULL LATITUDE COVERAGE

NOISE FREE CASE

Component	52^{0}	45^{0}	30^{0}	28^{0}	15^{0}	Orbital Inclinations
G_{21}	2.1	13.3	1657.9	2133.6	6612.6	
G_{22}	47.1	55.9	336.2	1036.0	6661.6	
H_{22}	11.7	48.2	77.7	2.5	115.5	
G_{31}	68.5	214.5	1610.5	1822.2	751.1	
G_{32}	5.8	12.7	285.6	527.2	5227.6	
H_{32}	1.1	15.4	420.1	483.9	8780.3	
G_{33}	9.3	28.4	266.0	248.8	5656.8	
H_{35}	42.8	68.2	120.5	170.7	530.9	
	3.0	3.01	15.7	18.2	34.5	RMS DEVIATION OF TOTAL 12^{0}x12^{0} FIT

UNITS NT

TABLE 2

INFLUENCE OF NOISE ON THE STATIC TERMS

COEFFICIENTS (52^{0})	$\lvert\Delta$ (NOISE FREE - 6 NT NOISE)$\rvert$
G_{21}	4.4
G_{22}	4.0
H_{22}	12.5
G_{31}	12.3
G_{32}	0.2
H_{32}	1.2
G_{33}	3.7
H_{33}	3.4
σ	0.4

UNITS NT

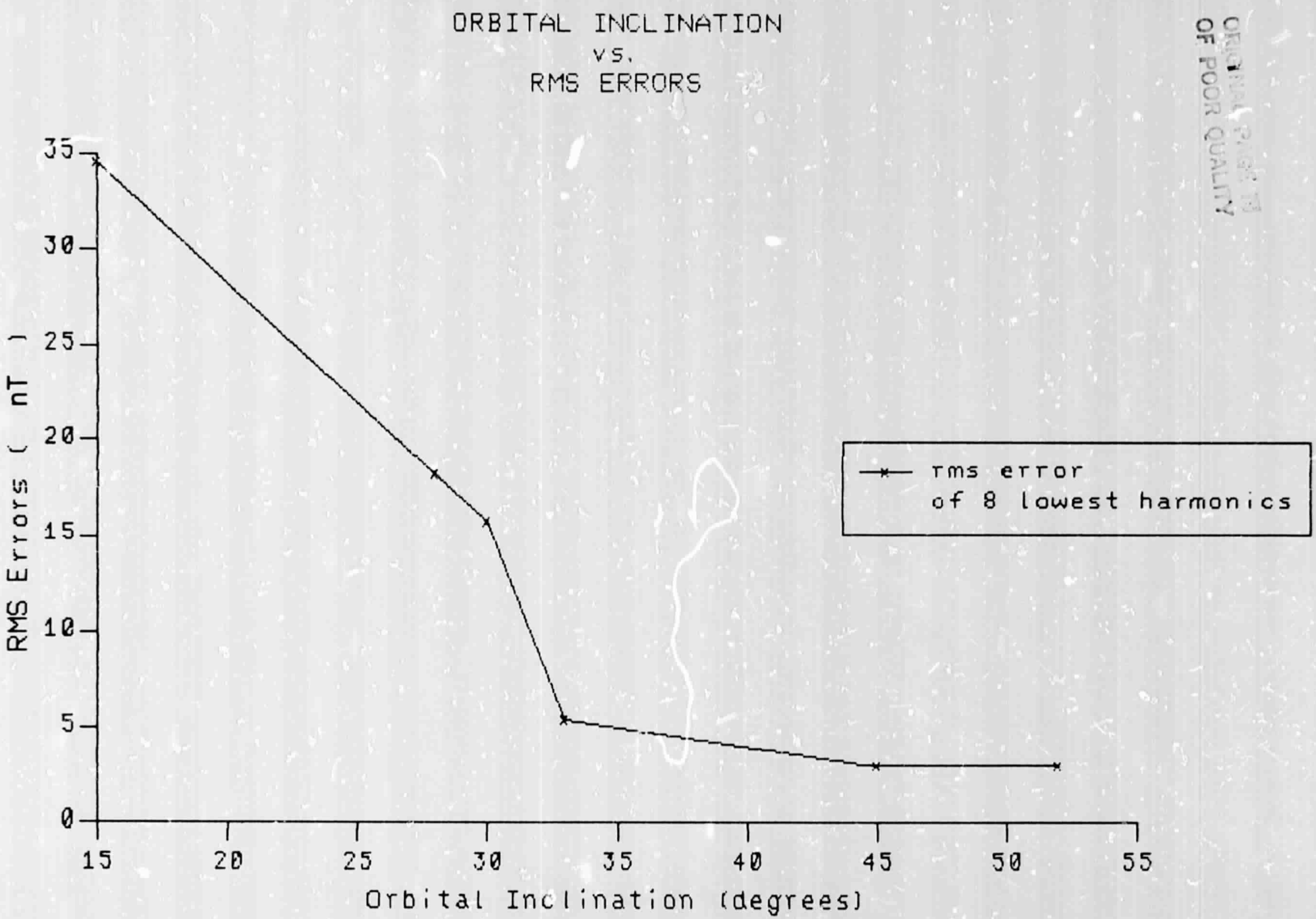
ORBITAL INCLINATION
vs.
RMS ERRORS
RMS Errors (nT)
35
30
25
20
15
10
5
0
15
20
25
30
35
40
45
50
55
Orbital Inclination (degrees)
rms error
of 8 lowest harmonics

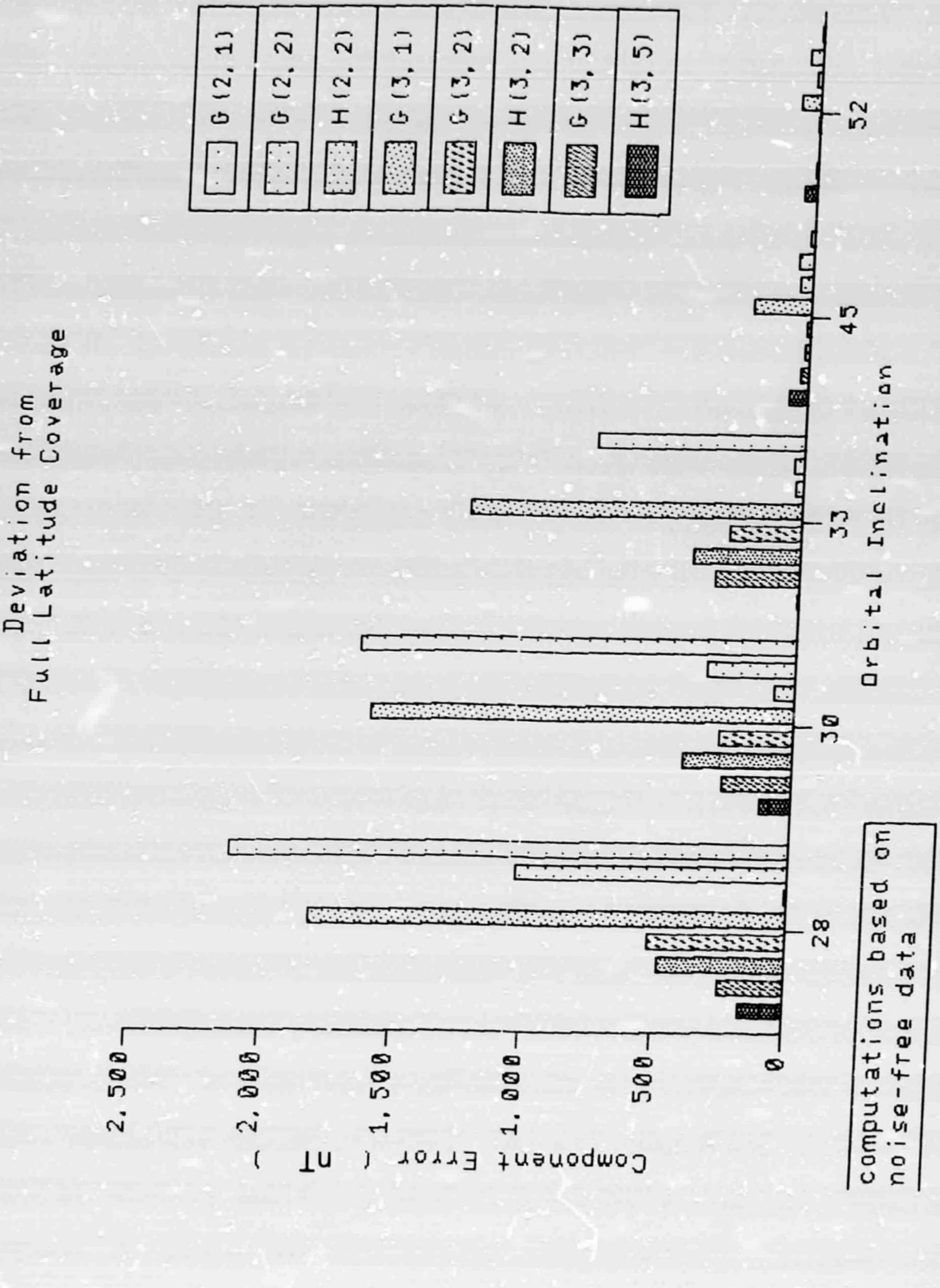
Deviation from
Full Latitude Coverage
Component Error (nT)
2,500
2,000
1,500
1,000
500
0
28
30
33
45
52
Orbital Inclination
G(2,1)
G(2,2)
H(2,2)
G(3,1)
G(3,2)
H(3,2)
G(3,3)
H(3,5)
computations based on
noise-free data

the results of Table 1 as a bar chart. This shows the general decline in the component errors with inclination.

When noise is introduced, the behavior with inclination remains similar in functional form. However, as would be expected, the addition of noise changes both the coefficient deviations and the rms error of the fit. In Table 2, we give the deviations for the 52° inclination case and 6 nT random noise. It is of interest to note that the representation error is slightly more than half the noise added (3.4 nT) and that most of the deviations increased by about 3.5 nT. However, note that H_{22} and G_{31} showed deviations which increased by twice the noise added.

The final analysis in this section concerns the ability to simultaneously recover both the static and time terms from the measurements. The assumed 6 nT noise is typical of the non-instrument noise in the Magsat observations. The fits reported here included 12 static terms (as before) and 7 time terms. Further, it was assumed that the time variation of the coefficients was linear.

It should be noted that we are presuming that the time terms are determined solely from the observations. Other than an a prioi estimate of the time terms, no other constraints have been applied.

In Table 3, we show the deviations and the rms errors of the representation. The general pattern observed in the noise free case remains (Table 3), although the best rms has increased from about 3 to about 11. Numerical experiments indicate that the increase in statistical degrees of freedom provided by the additional time terms, together with the additional statistical leverage provided by the inclusion of time variation in the data has produced a representation whose rms error estimate is more "honest" than the noise free case. In Figures 3 and 4 we give the same material as bar charts for the static and

TABLE 3

ABSOLUTE DEVIATIONS WITH 6 NT

(12 STATIC AND 7 TIME TERM ORDERS)

COEFFICIENTS	52^{0}	45^{0}	33^{0}	30^{0}	28^{0}	15^{0}	INCLINATION
STATIC							
G_{21}	6.59	312.9	4649.1	5693.7	8149.5	4196.6	
G_{22}	61.8	265.7	855.3	922.3	665.6	344.6	
H_{22}	143.0	310.6	514.7	469.2	637.9	555.8	
G_{31}	59.9	56.7	510.7	1859.0	1482.2	781.4	
G_{32}	24.2	68.4	156.5	241.2	365.0	10448.3	
H_{32}	7.5	17.4	479.2	730.0	1050.6	4124.2	
G_{33}	29.3	64.6	328.7	287.1	239.0	1869.3	
H_{33}	82.2	107.7	251.1	256.5	183.0	2036.2	
TIME VARIATION							
$\dot{G}_{21}$	0.7	6.3	3.7	8.3	2.9	7.3	
$\dot{G}_{22}$	5.5	8.1	12.1	18.2	11.3	52.6	
$\dot{H}_{22}$	0.1	4.8	13.8	13.0	26.6	60.0	
$\dot{G}_{31}$	2.4	15.0	95.6	137.6	189.2	101.3	
$\dot{G}_{32}$	1.3	4.2	13.7	13.4	10.3	35.0	
$\dot{H}_{32}$	0.6	3.6	26.0	39.0	51.1	31.9	
$\dot{G}_{33}$	1.5	5.9	17.2	22.4	22.5	39.1	
$\dot{H}_{33}$	5.1	8.7	16.7	16.4	8.5	8.0	
RMS	11.4	14.0	23.6	39.8	76.1	224.0	

UNITS NT

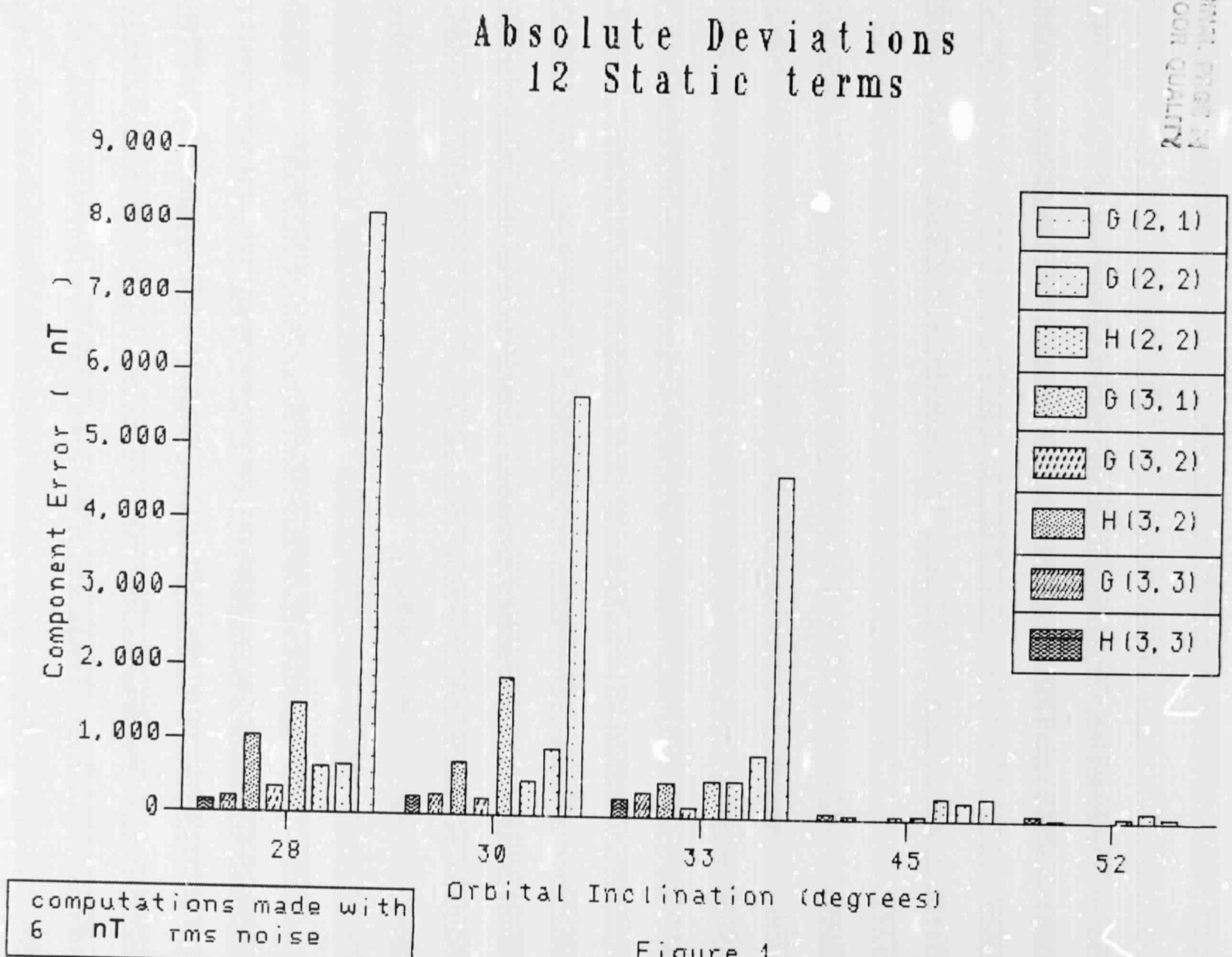
Absolute Deviations
12 Static terms
Component Error (nT)
9,000
8,000
7,000
6,000
5,000
4,000
3,000
2,000
1,000
0
28
30
33
45
52
Orbital Inclination (degrees)
G (2, 1)
G (2, 2)
H (2, 2)
G (3, 1)
G (3, 2)
H (3, 2)
G (3, 3)
H (3, 3)
computations made with
6 nT rms noise

Figure 1

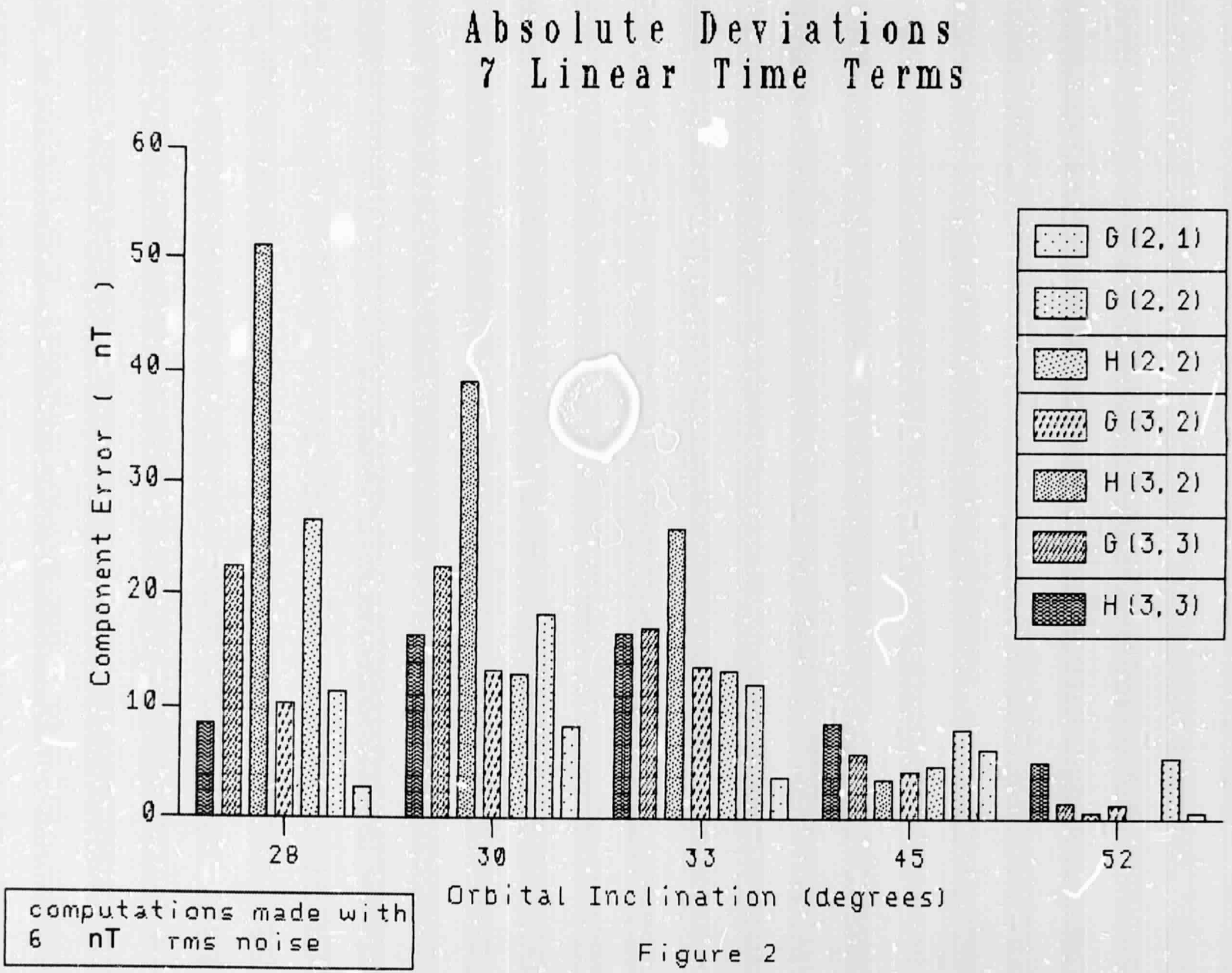

Absolute Deviations
7 Linear Time Terms
Component Error (nT)
60
50
40
30
20
10
0
28
30
33
45
52
Orbital Inclination (degrees)
G (2, 1)
G (2, 2)
H (2, 2)
G (3, 2)
H (3, 2)
G (3, 3)
H (3, 3)
computations made with
6 nT rms noise

Figure 2

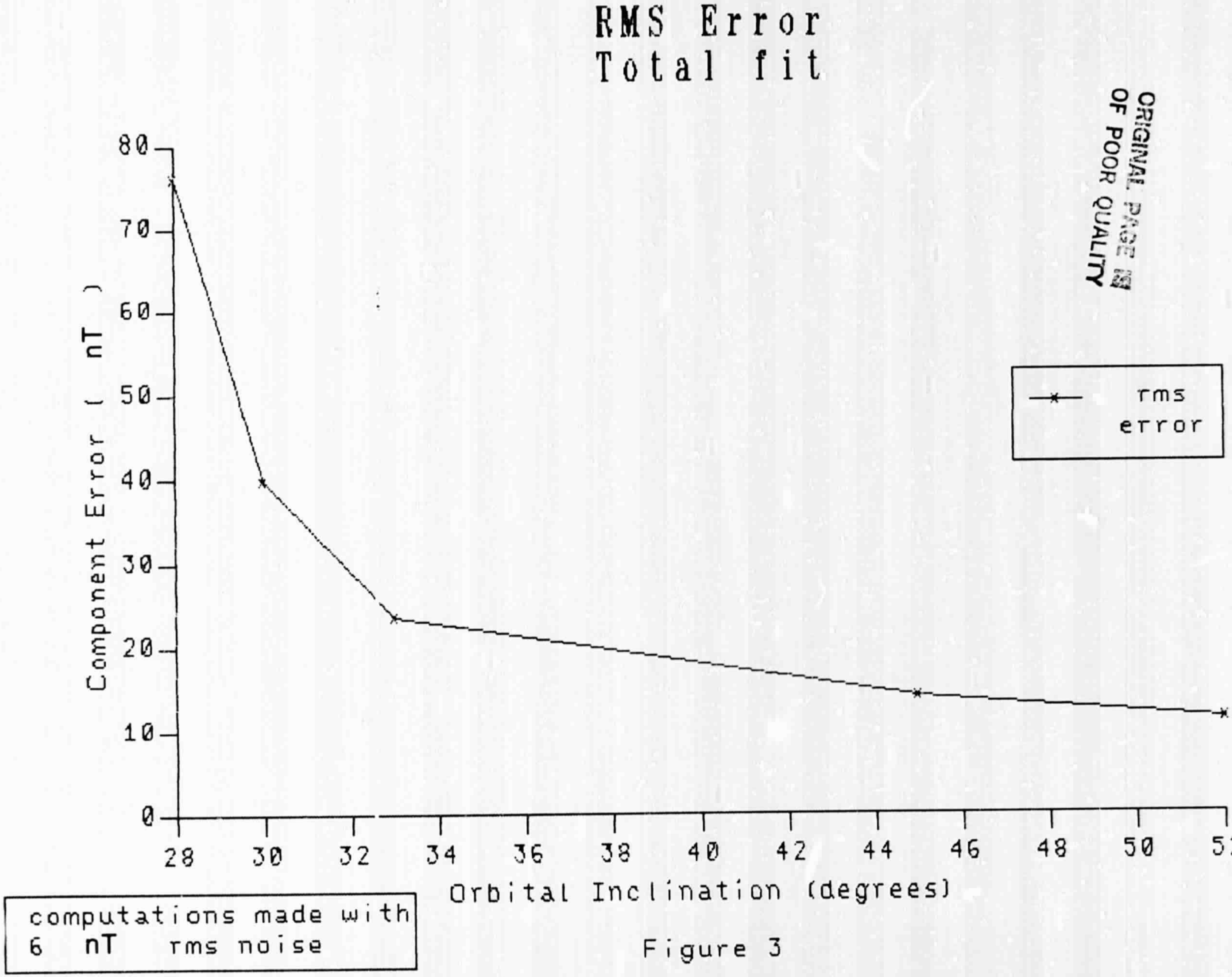
RMS Error
Total fit
Component Error (nT)
80
70
60
50
40
30
20
10
0
28
30
32
34
36
38
40
42
44
46
48
50
52
Orbital Inclination (degrees)
rms error
computations made with
6 nT rms noise

Figure 3

time terms separately. Figure 5 shows the dependence of the rms error of the representation on the inclination of the measuring orbit.

We are now in a position to assess the importance of the measuring orbit. It is clear that inclinations below 33° are not suitable for core field measurements. The static terms are very poorly determined and, except for the time term corresponding to the dipole moment, the time terms are also very poorly determined. The indicated deviation in the $\dot{G}_{21}$ term is low enough that a useful, although crude, estimate is possible for inclinations below 33°.

Clearly, as discussed earlier, the best determination will be made from the highest inclination of the measuring orbit. It seems clear that, while inclinations above 33° are suitable, a large change in inclination is required to gain a significant improvement in quality. That is, the improvement in going from 33° to 43° is not very great. One needs to go to 50° to see a major improvement over 33°. An inclination corresponding to a possible spacelab orbit (52°) produces a model quality which is quite suitable for a Magsat-accuracy determination (4 nT rms error).

We next address the question of how well the orbital position must be known. It should be pointed out that the need for position knowledge is a posteriori. The location of the measurement is usually tied to the data after the fact. This is most often done by calculating the position from very precisely determined orbital elements. These elements are usually determined by doppler, laser and radar measurements made at frequent intervals from a wide range of geographic locations.

The usual way to specify the required orbit accuracy is to specify a rectangular solid within which the spacecraft must be found. This solid has its axes in the along-track, cross-track and radial directions. This specification will be derived next.

The methodology for this analysis has been detailed by Langel (1976). Using a model for the main field, the gradients in the radial, along- and cross-track directions are calculated for the field components under consideration at the altitude of interest. Then, given the expected tracking accuracy, one can calculate the expected error in the component in question.

As in the previous section, we will be concerned with the scalar field. We will also use the MGST-481#2 model as before. Tracking accuracies will be adopted which are typical (300 m along- and across-track, 60 m radial). In Table 4, we give the calculated maximum gradients between $\pm 60^{\circ}$ latitude at 200 km altitude. Using the errors corresponding to the best results, the tabulated value of error in the scalar field (1.85 nT) results. To illustrate the variations with altitude, tracking error and latitude, we give in Table 5 the dependence of the error in the scalar field as a function of latitude for two altitudes and two different sets of tracking error.

This analysis makes it clear that the limiting factor in the ability to measure the scalar field is clearly not the instrumentation. With 3 to 0.5 nT being typical of the instrumental performance (Farthing, 1980; Acuna, 1980), the highest quality tracking is required to keep this error source comparable to or less than the instrumental noise. In practice, non-instrumental noise dominates the measurements.

The final question to be considered in this section is the required separation between the station and the magnetometer to limit the station's influence on the measurements.

TABLE 4

SCALAR FIELD ERROR AT 200 KM

	VERTICAL	ALONG TRACK	CROSS TRACK
MAXIMUM GRADIENT (NT/KM)	-30.3	-10.0	+13.3
TRACKING ERROR (M)	60	100	100
COMPONENT ERROR (NT)	3.0	1.0	1.33

SCALAR FIELD ERROR 1.85 NT

TABLE 5

INFLUENCE OF TRACKING ACCURACY ON FIELD MEASUREMENTS

ALTITUDE	160 KM	100 KM	100 KM
TRACKING ACCURACIES			
ALONG TRACK:	300 M	300	100
CROSS TRACK:	300	300	100
RADIAL:	60	60	30
LATITUDE BAND			
60	3.8	4.5	1.5
50	4.0	4.6	1.5
40	4.0	4.5	1.5
30	4.0	4.2	1.5
20	3.5	3.6	1.3
10	2.8	2.9	1.0
0	1.9	2.0	0.7
-10	2.8	3.0	1.1
-20	3.4	3.7	1.3
-30	4.0	4.2	1.5
-40	4.3	4.2	1.6
-50	4.3	4.3	1.6
-60	4.3	4.0	1.6

UNITS NT

Any object composed of most metals and/or carrying an electric current will be surrounded by a magnetic field. High frequency components of this field are not a problem, however. The true temporal variations as well as the apparent temporal variations due to orbital motion are all of relatively low frequency. Accordingly, variations at a rate greater than a few hundred hertz are not "real" and are ordinarily suppressed by filtering. However, the fields due to low frequency currents mimic the apparent temporal and spatial variations of the real field.

The low and zero frequency currents are thus the most troublesome. In the case of unmanned spacecraft, careful shielding with magnetic barrier materials and routing currents so that the fields tend to cancel are required. Even when the greatest care is taken to suppress the low frequency fields, it is still necessary to deploy the magnetometer sensor-head a considerable distance from the spacecraft main-body. The use of distance to attenuate spacecraft fields at the sensor has proved essential even in those cases where extreme measures have been taken to suppress spacecraft fields. In the case of Magsat, it was necessary to place the magnetometer sensor head on a 6 meter boom to drop the spacecraft fields under 0.5 nT at the sensor.

It is not reasonable to expect that the stray fields surrounding the space station can be controlled to the extent of the stray fields around Magsat. Accordingly, we must consider displacing the magnetometer much more than 6 meters from the station. We are, therefore, considering a free flyer which is to be displaced a minimum distance from the station. This minimum distance will depend on the DC magnetic moment of the station.

Obviously, a precise value of the magnetic moment can only be calculated when one knows the shape of the station and the distribution of currents in

TABLE 6

DISTANCE	0°	20°	40°	80°	90°
50	.25E02	.26E02	.30E02	.48E02	.50E02
100	.20E03	.21E03	.24E03	.38E03	.40E03
150	.67E03	.70E03	.81E03	.13E04	.13E04
200	.16E04	.17E04	.19E04	.30E04	.32E04
250	.31E04	.33E04	.37E04	.60E04	.62E04
300	.54E04	.56E04	.65E04	.10E05	.11E05
400	.13E05	.13E05	.15E05	.24E05	.25E05
500	.25E05	.26E05	.30E05	.48E05	.50E05
700	.68E05	.71E05	.82E05	.13E06	.14E06
1000	.20E06	.21E06	.24E06	.38E06	.40E06
1500	67E06	.70E06	.81E06	.13E07	.13E07
2000	.16E07	.17E07	.19E07	.30E07	.32E07
2500	.31E07	.33E07	.37E07	.60E07	.62E07

the electrical and electronic systems. For the present, a design tool is needed which will yield a conservative estimate for the required separation.

We have chosen to provide this estimate by means of the DC magnetic dipole moment. For a magnetic cylinder of specified dipole moment, we calculated the distance from the surface of the cylinder required to drop the scalar field to 0.5 nT as a function of the angle between the major axis of the cylinder and the observation direction. From these calculations, we have prepared a table which summarizes the results. Table 6 is used as follows: for a given configuration estimate the dipole moment in Ampere-meter^2 units. Next select an angle with respect to the major axis of the station. Go down the corresponding column until to the moment nearest the desired value (round upwards as needed). Now follow the resulting row to the left to find the distance. As an example, for a moment of 1.1×10^5 Am^2 at an angle of 20°, a separation of 800 m is required (typical space shuttle orbiter).

Low Altitude Observations

We will adopt ground rules similar to the previous section here. However, since we are considering, as we shall see, a manuverable free flyer, considerations of reasonable propulsion capability, restrict our analysis to orbits roughly co-planar with the station. Because we want to be able to service the low altitude system and to control its operation from the station (which will likely be in a low-28°5-inclination orbit), we have eliminated polar orbits from consideration. A previous study (Webster 1983) has shown that there are decided advantages to observing the crustal field from a non-polar orbit even though global coverage is lost.

The low altitude observations are directed toward observations of the crustal component of the earth's magnetic field and in situ measurement of the magnetic properties of the low-latitude portion of the earth's current system, especially the equatorial electrojet.

In addressing the observations of these two components, we must consider the following questions:

1. What is the lowest altitude at which useful observations can be made? Spacecraft which operate in the 90 to 120 km are normally beginning reentry. Under 100 km, the plasma column is intense enough to block radio transmissions. Somewhere between 80 and 120 km, the magnetic noise of the plasma becomes intense enough to screen out external fields.

2. How can the characteristics of the equatorial electrojet be best determined? Typically, the electrojet spans the altitude range from about 90 to 110 km. Therefore, observations will be made outside as well as within the jet. How shall the jet's influence be detected? What instrument complement is required?

3. What level of improvement over previous data can be expected from a non-polar, low-altitude orbit? Portions of this problem have been treated in a previous study whose results will be summarized here.

Note that the required accuracy of orbit determination has been treated in the previous section.

The lowest altitude at which the crustal field can be detected depends on the electron content of the sheath around the spacecraft and the variations in the electron content. A previous study established that the plasma content of the wake can be a significant problem even at shuttle altitudes (Webster, 1983). At the lower altitudes employed by the Atmospheric Explorer series of manuverable satellites, aerodynamic heating was a signficant design consideration (Caruso and Nageli, 1976) and the formation of a reentry shock made interpretation of lowest altitude measurements uncertain.

Although the Atmospheric Explorer satellites (especially AE-C) carried fluxgate vector magnetometers as part of the instrument complement, the analysis of these measurements was severely compromised by the necessity to mount the sensor head on the surface of the spacecraft, resulting in ±40 nT rms noise (Bythrow et al., 1980). Although these data are of great value in studies of the polar current system (Bythrow et al., 1981) they are not sufficient to define the extent of screening observed. Accordingly, we have resorted a theoretical calculation based on a model atmosphere to gain some insight into the screening.

Atmospheric models in the 90 to 150 km range are usually averages over a wide range of conditions. In our case, we have elected to use the Hedin (1979) models of the upper atmosphere as these are derived from a consistent set of repeated measurements with the same kinds of instruments (satellite and ground based). The Hedin (1979) models cover the thermospheric region (from 120 to 800 km altitude) as a function of 10 cm scalar radio flux, season, latitude, local time and level of magnetospheric disturbance. In order to obtain values in the 90 to 120 km region we extrapolated from the 120 to 150 km region using the hydrostatic equation. The quality of this extrapolation was checked by comparing the results with the standard atmospheres in the Handbook of Geophysics and Space Environments (1970).

Having values of the mass density, temperature pressure and chemical composition, it is now possible to calculate the ionic content of the wake and bow wave surrounding the spacecraft. What is calculated is the fractional ionization of the components of the gas and from this the equivalent current density. Once the current density is calculated, the disturbing field follows from Maxwell's equations. The magnitude of the disturbing field compared with the strength of the crustal field at the altitude of observations gives the screening effectiveness.

The fractional ionization resulting from the formation of the wake can be calculated for each of the species by using the models, and measurements used to predict the performance of the shuttle control and thermal protection systems (Greenwood et al., 1983; Goodrich et al., 1983). From this, the total electron content of the wake and the disturbing field follow directly for each model atmosphere. In Table 7, we give the results of these calculations. It is obvious that the screening below 100 km is going to make it impossible to observe the crustal field under virtually all conditions.

We now consider the measurement of the electrojet characteristics. For a review of the current understanding of the electrojet, see the review article by Forbes (1981). The equatorial electrojet is that part of the earth's current system which follows the geomagnetic equator. It is relatively confined in geomagnetic latitude and has a half-current width (E-W component) of about 4° centered on the geomagnetic equator. The jet has a complex current structure which, in addition to a local solar time variation, shows both meridional and latitudinal current flow. In addition, the flow of charge is irregular, depending on very high altitude winds and solar activity.

The jet typically covers the altitude range from about 90 to 130 km with an observed half-current density width of about 15 km. The effects of the jet on high altitude observations were clearly evident in the Magsat measurements (Maeda et al., 1982) made at an altitude well above (350 km) the actual jet. This occurred even though the Magsat orbit was chosen to be always at local twilight in order to minimize the effects of the jet and

TABLE 7

CALCULATED SCREENING FACTORS

	Screening Factor		
ALTITUDE	MINIMUM	MAXIMUM	NOTES
120 KM	1%	1%	SOME GLOW OBSERVED ON SHUTTLE SURFACES
110 KM	5%	6%	
100 KM	9%	11%	
95 KM	93%	100%	
90 KM	95%	100%	COMMUNICATION BLACKOUT BEGINS AT 95 KM FOR STS

other equatorial currents.

An orbit with an inclination different from Magsat's (sun synchronous) will see a much stronger field perturbation due to the currents. Further, observing at around 100 km guarantees that the instrument package will enter the most intense part of the current system on a regular basis. Accordingly, the low altitude observations contemplated here will provide an unparalleled opportunity to study the equatorial current system in situ.

The direct measurement of the properties of the equatorial current has usually been performed by sounding rockets. Early on (Cahill, 1959), magnetometers were included in these payloads. Given a few simple assumptions, it is straightforward to invert the magnetic measurements for the current density (Davis et al., 1971). Rocket observations showed a change of about 225 nT in about 30 km in the geographic region off the west coast of South America. In other geographic regions, scalar derivatives much larger than this have been reported. Typically, maximum current densities of 10 amp/km^2 have been inferred at the peak of the jet.

Since the current generated fields have finite curls and since the crustal anomaly fields are curl free, the current contribution can be distinguished by its deviation in direction from the induced crustal field. Accordingly, while a scalar magnetometer appears to be sufficient for the study of the crustal field, a vector magnetometer is required to separate the jet field from the other components.

Models of the equatorial current system are now available which evidence considerable sophistication (Sugiura and Poros, 1969; Kisabeth, 1979; Akasofa et al., 1980) and appear to be in accord with the broad scale, snapshot observations available to date. Although some of these models are given as calculated vector magnetic fields, most results are presented as current density distributions. Accordingly, in order to get some indication of the field to be expected, we have included as Appendix 1, the Fortran code for a calculation of the expected field due to a model jet current distribution. As included, the program is set up for the Suigura and Poros (1969) model and calculates the observed fields using the "sounding rocket approximation" for a longitude cut through the current system. The sounding rocket approximation (Cahill, 1959) uses plane-parallel current sheets and relatively large layer spacings to infer the current density distribution from the magnetometer data. We have chosen to invert that process here. Although most modern (i.e., Akasofu et al., 1980) analyses are considerably more sophisticated, the approximation is a useful tool for preliminary planning.

Evidence has also been accumulating which shows that there are substantial fluctuations in velocity and density (see Forbes, 1981). Although these variations will probably not compromise the instrumentation, it may prove necessary to correct for an additional orbital decay introduced by the increased drag. The fluctuations and the mechanisms which maintain them are of considerable interest in understanding the structure and evolution of the electrojet.

We now consider the improvement over existing measurements of the crustal component to be expected from the kind of observations we propose here. This section is summary and extension of a previous study (Webster, 1983).

Observations made near 100 km and from a non-polar orbit have two advantages over the Magsat observations. The clearest is, of course, the substantially lower altitude. We will discuss this below. A more subtle advantage accrues from the non-polar orbit.

Magsat was intended, among other things, to give global-coverage observations of the crustal magnetic field from an orbit which minimized the influence of the current system. The particular orbit selected was sun-synchronous with dawn and dusk equator crossings and, although the equatorial currents were not totally invisible, it was possible to map the crustal field in the equatorial region both in total field and vector components.

If one is prepared to sacrifice global coverage and accept a stronger and more time variable contribution from the equatorial current system, it is possible to take advantage of the different perspective provided by a non-polar orbit.

As is shown in Webster (1983), the analysis required to recover the crustal field from the observations results in the unavoidable suppression of long, along-track structures. This suppression results from, among other things, the need to remove the residual effects of the current system down to very low spatial frequencies.

The result of this suppression in the case of Magsat is to eliminate north-south trending structures with lengths greater than about 1900 km and to attenuate structures in the 1500 to 1900 km range with increasing severity (Sailor et al., 1982). Accordingly, one does not see, nor does one expect to see major magnetic sources ascribable to the mid-Atlantic Ridge, the Rocky Mountains, the Appalachian Mountains or the Andes Mountains, among other N-S trending features, in the Magsat maps.

It is clear that observations at an inclination very different from sun-synchronous polar (around 97^{o}) will provide a complementary view of the crustal field.

The effects of lower altitude have been quantified by Taylor (1982) we illustrate the effects on resolution and source strength in Figures 6 and 7. These figures are the calculated anomaly fields for a 20^{o} long (longitude), 0.5^{o} wide (latitude) body extending from the surface to 20 km depth and showing a magnetization contrast of 0.003. The contour interval is 2 nT. Figure 6 was calculated for 160 km while Figure 7 was calculated for 100 km.

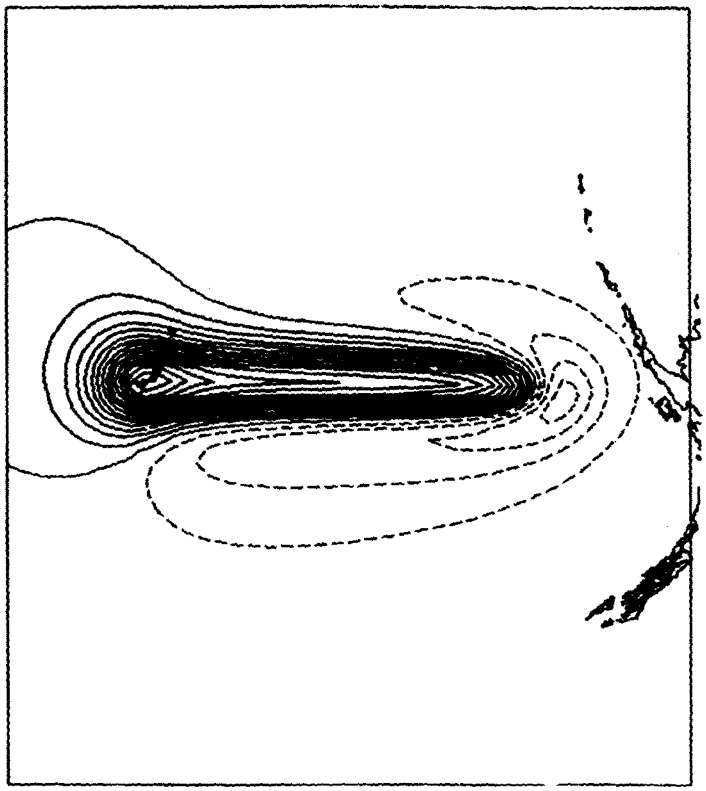

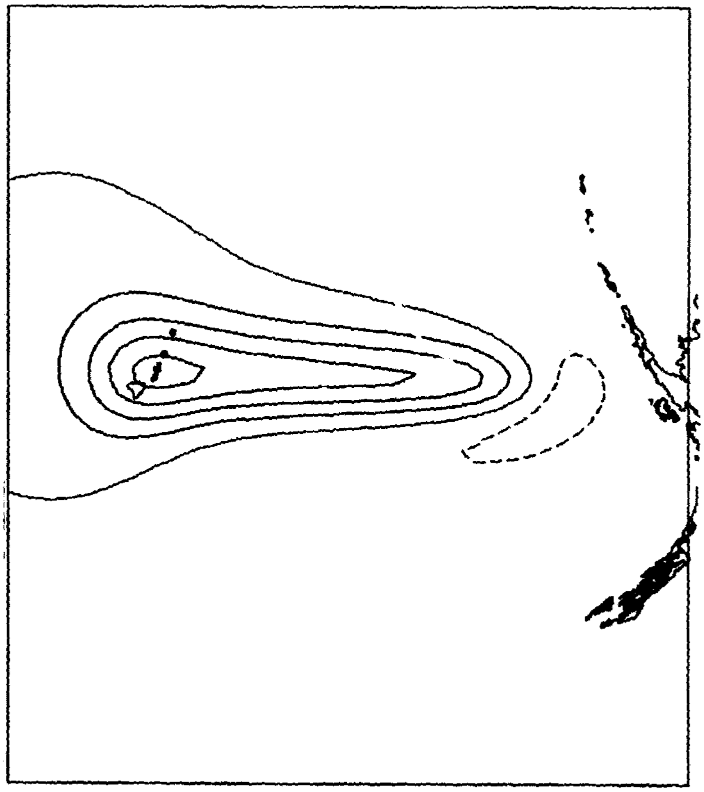

In neither case is the 0.5^{o} width in latitude resolved. However, the half intensity width in latitude of Figure 7 is a factor of 1.5 less than for Figure 6. The peak intensity in Figure 7 is 3.5 times the peak intensity in Figure 6. These figures show that, qualitatively, it is clear that significant improvements can be expected from the lower altitude. The work by Taylor (1982) provides quantitative estimates and the reader is referred to that work.

Mission Scenarios and Operational Requirements

The two kinds of observations require very different levels of involvement. The high altitude observations can be thought of as a monitoring activity. Therefore, the level of space station crew involvement is relatively modest. However, with a duration of tens of years for the observations, maintenance, repair and calibration became of supreme importance.

The high altitude observations can be used for more purposes than we have discussed here. For example, they can be used to decide if the radiation environment could become severe enough to require protection of the crew or instruments. In addition, these observations are crucial in deciding whether the level of magnetospheric activity warrants the low altitude observations.

The prime purpose of the high altitude observations is, however, the measurement of the low order moments of the main field and the determination of the temporal spectrum of the secular variation. In order that this be accomplished an attention to long term effects is required which has not been necessary previously. In all previous experiments, the duration of measurement has been a year or two at most. There is, therefore, not much experience in long duration, precisely calibrated instruments in space.

There is, however, a body of experience which seems to be applicable. Although the environment is different and in some ways (vibration, etc.) more hostile than space, airborne magnetometer observations taken in petroleum exploration are in many ways analogous to our problem. Petroleum exploration groups are concerned with field mapping, either scalar or vector, with a sufficient percision to allow the linking of surveys taken at different times over adjacent locations. This level of precision is comparable to what we require. The major environmental difference is, of course, that an airborne instrument suffers a much more severe vibration environment than a space station based instrument would experience. Nonetheless, this experience is valuable in assessing the routine maintenance and calibration required.

In Tables 8 and 9, we summarize the routine procedures used by Phillips Petroleum Company (H. Tiedemann, personal communication) in maintaining their airborne instruments. It is not surprising that a considerable amount of effort is involved in maintaining a fluxgate instrument at the required levels. It may, however, be surprising to see the level of effort involved in maintaining an atomic constant instrument. Atomic constant instruments are absolute magnetometers. That is, the field is determined from the measurement of the charge of a fundamental atomic or molecular property, usually a transition frequency. It is the measurement of this property which must be precise and accurate. In the case of the cesium vapor magnetometer used on Magsat (Farthing, 1980) the measurement was of an oscillation frequency in a combined RF/optical feedback loop. The counter (or tracking filter) must have sufficient accuracy and precision to make the required measurement for (in our case) a long time.

The considerations outlined above also apply to the low altitude observations. In this case, the free-flyer would be operating only for relatively short

TABLE 8

FLUXGATE INSTRUMENTS (USUALLY VECTOR)

BEFORE EACH FLIGHT

- MEASURE HYSTERESIS CURVE OF EACH AXIS
- CHECK LINEARITY OF OFFSET CURRENT GENERATOR
- TEST RESOLUTION OF DATA SYSTEM
- VERIFY TIMING AND CONTROL LOGIC PERFORMANCE

AT THE BEGINNING AND END OF EACH SERIES

- VERIFY AXIS ALIGNMENT USING ALIGNMENT TOOL
- VERIFY PERFORMANCE WITH "STANDARD" ELECTROMAGNET

AT YEARLY INTERVALS

- FULL OPTICAL ALIGNMENT CHECK OF AXES
- HELMHOLTZ COIL CALIBRATIONS

TABLE 9

ATOMIC CONSTANT INSTRUMENTS (USUALLY SCALAR)

BEFORE EACH FLIGHT

- CHECK LAMP CURRENT AND FREQUENCY
- VERIFY EXISTANCE OF OSCILLATION OF MAGNETOMETER
- CALIBRATE PRECISION AND ACCURACY OF DIGITAL COUNTER SYSTEM

AT THE BEGINNING AND END OF EACH SERIES

- MEASURE TRANSPARENCY OF OPTICS, PRESSURE IN CELLS
- CHECK LINEARITY AND SENSITIVITY WITH "STANDARD" MAGNET

AT HALF-YEARLY INTERVALS

- SIDE-BY-SIDE COMPARISON WITH OBSERVATORY INSTRUMENT periods at 100 km. Since it will obviously take time to map the crustal field at 100 km, the low altitude instrument must be maintained to a comparable level. In fact, the operation in a manuverable spacecraft in a near-reentry trajectery undoubtedly stresses the instrument to as high a degree as aircraft operations.

We now examine the mission scenarios for the two kinds of observations. As we have previously observed, observation of the main field from relatively high orbit is not a labor intensive task. Table 9 lists the kinds of tasks which would have to be performed in concert with observations. The anticipated data rate and volume is sufficiently low that major portions of the data reduction and analysis could be performed on the station. Data rates are likely to be of the order of 10 kbs including housekeeping and command and control. At these data rates it is practical for a small, general-purpose computer to calibrate the data and produce displays of "todays field" as a background job.

The low altitude observations need a much greater level of involvement than the high altitude observations. Because this system is fully manuverable, it must be refueled and maintained on a frequent schedule. Further, although the descent from the station and the ascent to the station after operations can clearly be done without human control or monitoring, operations at low altitude will have to be monitored and controlled in real time. At operating altitude, aerodynamic heating and drag are of sufficient importance that they must be continuously watched and the various applied forces compensated for. In Table 10, we summarize these and other considerations.

TABLE 10

<u>ROUTINE MONITORING OF THE MAIN FIELD FROM "HIGH" ORBIT</u>

$I \sim 55^{0}$

$A \sim 200$ KM

INSTRUMENT: ABSOLUTE VECTOR MAGNETOMETER, 0.5 NT RMS INSTRUMENT/SPACECRAFT NOISE

- REVISITS FOR REPAIR AS NEEDED
- ROUTINE MAINTENANCE (PROBABLY HALF-YEARLY BASIS)
- DATA "QUALITY" CHECKING REQUIRED TO SELECT INTERVALS SUITABLE FOR FIELD MODEL DETERMINATION AND SECULAR VARIATION DETERMINATION (NOT NECESSARILY REAL-TIME)
- CHECKS ON CURRENT SYSTEM SIGNATURE AND LEVEL OF DISTURBANCE TO PLAN LOW ALTITUDE DATA COLLECTION

TABLE 11

LOW ALTITUDE OBSERVATIONS OF THE CRUSTAL FIELD AND ELECTROJET FIELD

A ~ 100 KM

I AS AVAILABLE

INSTRUMENT: SCALAR MAGNETOMETER, 0.5 NT RMS INSTRUMENT/ SPACECRAFT NOISE

- NEAR-REAL TIME MONITORING AND CONTROL REQUIRED DURING LOWEST ALTITUDE OPERATIONS
- OPERATION AT LOW ALTITUDE AS FULL FREE-FLYER OR ALTITUDE-STABILIZED, TETHERED SATELLITE
- PENETRATE THE EQUATORIAL ELECTROJET AT VARIOUS LOCAL SOLAR TIMES
- MEASURE THE CRUSTAL FIELD AWAY FROM THE JET

The Space Station as a Measurement Base

This study has shown that measurement of the earth's magnetic field by means of a low-altitude, manuverable free-flyer and a high-altitude, non-manuverable free-flyer can contribute to a major improvement in our understanding of the core, crustal and electrojet components of the earth's magnetic field. In operating and deploying these systems, the availability of the space station and its resources results in a higher reliability, longer duration and greater scientific benefit from the data.

Clearly, the kinds of measurements proposed here could be done in a number of ways. The high altitude measurements might, for example, be made by a conventional unattended satellite. However, the availability of the space station as a staging base alone makes for economics not possible with conventional technqiues.

The high altitude observations must be conducted for 5 years at a minimum. The greatest scientific benefit will accrue if the observations continue for more than a decade. Clearly, this operating environment is greatly different from conventional satellite magnetometry. Only the deep space probes (Voyager, Pioneer) have approached this kind of operating lifetime.

As we have reported above, the operation which best approximates the high altitude measurements has a considerable amount of built-in preventative maintenance. It is apparent that an extended operation cannot be conducted effectively without the regular preventative maintenance. In addition, unless a vector absolute magnetometer can be constructed, regular recalibration will be required. All of these operations could be conducted by shuttle launched from the ground. It should be obvious that conducting the mission this way would be exceedingly expensive. Accordingly, these measurements are not partical without the space station's capabilities.

Repetitive observations of the crustal field at low altitude also can be conducted in a number of ways. Whatever mechanism is selected, failure to make use of the station will drive the cost and degree of difficulty out of the realm of possibility. Although a few observations at low altitude could be performed by conventional technqiues, mapping the crustal field is not likely to be possible without regular refueling and preventative maintenance. It is clear that these observations also require the space station for their execution.

In summary, the actual measurements will be taken remote from the station. It could, therefore, be argued that the proposed systems are independent of the station. However, the using the station as a measurement base makes it possible to do the measurements in sufficient quality and over a sufficient time interval to obtain a maximum scientific benefit.

Bibliography

Acuna, M.H., 1980, The Magsat Precision Vector Magnetometer, ABL Tech. Digest, 1, 210.

Akasofu, S.I., Ahu, B.H. and Kisabeth, J., 1980, Distribution of Field. Aligned Currents and Expected Magnetic Field Perturbations from Auroral Currents Along Circular Orbits of Satellites, JGR, 85, 6883.

Backus, G.E., 1970, Non-Uniqueness of the External Geomagnetic Field Determined by Surface Intensity Measurements, JGR, 75, 6337.

Bythrow, P.F., Heelis, R.A., Hanson, W.B. and Power, R.A., 1980, Simultaneous Observations of Field-Aligned Currents and Plasma Drift Velocities by Atmospheric Explorer C, JGR, 85, 151.

------, 1981, Observational Evidence for a Boundary Layer Source of Dayside Region 1 Field-Aligned Currents, JGR, 86, 5577.

Cahill, L.J., Jr., 1959, Investigation of the Equatorial Electrojet by Rocket Magnetometer, JGR, 64, 489.

Caruso, P.S. and Naegeli, C.R., 1976, Theoretical and Empirical Low Perigee Aerodynamic Heating During Orbital Flight of an Atmospheric Explorer, in McKillop, A. (ed.), Proceedings of the 1976 Heat Transfer and Fluid Mechanics Institute, Stanford University Press: Palo Alto, California.

Davis, T.N., Burrows, K. and Stolarik, J.D., 1967, A Latitude Survey of the Equatorial Electrojet with Rocket-Borne Magnetometers, JGR, 72, 1845.

Estes, R.H., 1983, Fit Program Description and User's Guide Version 8305, Final Report NASA Contract NAS5-26486.

Farthing, W.H., 1980, The Magsat Scalar Magnetometer, APL Tech. Digest, 1, 205.

Forbes, J.M., 1981, The Equatorial Electrojet, Rev. Geophys. and Space Phys., 19, 469.

Greenwood, T.F., Lee, Y.C., Bander, R.L., and Carter, R.E., 1983, Calculation of Shuttle Base Heating Environments and Comparison with Flight Data, in Arrington, J.P. and Jones, J.J. (eds.), Shuttle Performance: Lessons Learned, NASA Conference Pub. 2283, p. 653.

Goodrich, W.D., Derry, S.M. and Bertin, J.J., 1983, Shuttle Orbiter Boundary Layer Transition at Flight and Wind Tunnel Conditions, IBID, p. 753.

Hedin, A.E., 1979, Tables of Thermospheric Temperature, Density and Composition Derived from Satellite and Ground Based Measurements, GSFC Laboratory for Planetary Atmospheres.

Kisabeth, J.L., 1972, On Calculating Magnetic and Vector Potential Fields Due to Large-Scale Magnetospheric Current Systems and Induced Currents in an Infinitely Conducting Earth, in Olson, W.P. (ed.), Quantitative Modeling of Magnetospheric Processes, AGU, Washington, D.C., p. 473.

Langel, R.A., 1974, Near-Earth Magnetic Disturbance in Total Field at High Latitudes, 1. Summary of Data for OGO 2, 4 and 6, JGR, 79, 2363.

------, 1976, Effects of Orbit Error on Satellite Magnetic Field Experiments, NASA/GSFC, X-922-76-124.

Maeda, H., Iyemori, T., Araki, T., and Kamei, T., 1982, New Evidence of a Meridional Current System in the Equatorial Ionosphere, GRL, 9, 337.

Sailor, R.V., Lazarewicz, A.R. and Brammer, R.F., 1982, Spatial Resolution and Repeatibility of Magsat Crustal Anomaly Data Over the Indian Ocean, GRL, 9, 289.

Stern, D.P., and Bredekamp, J.H., 1975, Error Enhancement in Geomagnetic Models Derived from Scalar Data, JGR, 80, 1776.

------, Langel, R.A. and Mead, G.D., 1980, Backus Effect Observed by Magsat, GRL, 7, 941.

Sugiura, M. and Poros, D.J., 1969, An Improved Model Equatorial Electrojet with a Meridional Current System, JGR, 74, 4025.

Taylor, P.T., 1982, Geopotential Research Mission-Magsat B Simulations, presented at Gravsat Users Data Analysis Working Group Meeting, June 30, 1982.

Webster, W.J., Jr., 1983, Observations of the Earth's Magnetic Field from the Shuttle: A Preliminary Examination of Shuttle-Based Observations of the Crustal Magnetic Field Using a Magsat Vector Magnetometer, NASA/GSFC, X-920-83-5.

Appendix

```
COMPILER OPTIONS - NAME=  MAIN,OPT=02,LINECNT=82,SIZE=0000K,
                   SOURCE,EBCDIC,NOLIST,NODECK,LOAD,MAP,NOEDIT,ID,XREF
                  C     INPUT STREAMLINE FUNCTION P AND ZONAL CURRENT RX
                  C      DEFINED ON Y-Z GRID
                  C     OUTPUT MAGNETIC COMPONENTS BX,BY,BZ ON SAME GRID
                  C     BY = DP/DZ , BZ = -DP/DY
ISN 0002              DIMENSION P(21,12),RX(21,12),BX(21,12),BY(21,12),BZ(21,12)
ISN 0003              DIMENSION Z(12),Y(21)
ISN 0004              M=21
ISN 0005              N=12
ISN 0006              DATA DY,DZ/100.,5./
ISN 0007              CC=4.*3.14159/10.
ISN 0008              RX(11,3)=40.
ISN 0009              RX(12,3)=40.
ISN 0010              RX(11,4)=30.
ISN 0011              RX(12,4)=30.
                  C     DBY/DZ=-4PI/10*RX
                  C     DBX/DY=-4PI/10*RZ=4PI/10*DP/DY
                  C     DBX/DZ=4PI/10*RY=4PI/10*DP/DZ
                  C     FROM THESE LAST TWO EQNS BX=4PI/10*P
ISN 0012              DO 10 I=1,M
ISN 0013              DO 20 J=2,N
ISN 0014              BY(I,J)=BY(I,J-1)-CC*DZ*.5*(RX(I,J-1)+RX(I,J))
ISN 0015              BX(I,J)=CC*P(I,J)
ISN 0016           20 CONTINUE
ISN 0017              BX(I,1)=CC*P(I,1)
ISN 0018           10 CONTINUE
                  C     COMPUTE BZ FROM DBY/DY+DBZ/DZ=0
ISN 0019              M1=M-1
ISN 0020              DO 30 I=2,M1
ISN 0021              DO 30 J=2,N
ISN 0022              DBY=.25*(BY(I+1,J-1)-BY(I-1,J-1)+BY(I+1,J)-BY(I-1,J) )
ISN 0023              BZ(I,J)=BZ(I,J-1)-(DZ/DY)*DBY
ISN 0024           30 CONTINUE
ISN 0025              DO 35 J=1,N
ISN 0026              BZ(1,J)=BZ(2,J)
ISN 0027              BZ(M,J)=BZ(M1,J)
ISN 0028           35 CONTINUE
ISN 0029              IM=(M+1)/2
ISN 0030              DO 40 I=1,M
ISN 0031              Y(I)=(I-IM)*DY
ISN 0032           40 CONTINUE
ISN 0033              DO 50 J=1,N
ISN 0034              Z(J)=90.+(J-1)*DZ
ISN 0035           50 CONTINUE
ISN 0036              WRITE(6,1)
ISN 0037            1 FORMAT('      BX COMPONENT',//)
ISN 0038            2 FORMAT('      BY COMPONENT',//)
ISN 0039            3 FORMAT('      BZ COMPONENT',//)
ISN 0040              WRITE(6,5)(Z(J),J=1,N)
ISN 0041            5 FORMAT('  ALTITUDE = ',12F5.0)
ISN 0042              DO 60 I=1,M
ISN 0043              WRITE(6,6)Y(I),(BX(I,J),J=1,N)
ISN 0044           60 CONTINUE
ISN 0045            6 FORMAT(' Y=',F9.0,12F5.0)
ISN 0046              WRITE(6,2)
ISN 0047              WRITE(6,5)(Z(J),J=1,N)
ISN 0048              DO 70 I=1,M
ISN 0049              WRITE(6,6)Y(I),(BY(I,J),J=1,N)
ISN 0050           70 CONTINUE
ISN 0051              WRITE(6,3)
ISN 0052              WRITE(6,5)(Z(J),J=1,N)
ISN 0053              DO 80 I=1,M
ISN 0054              WRITE(6,6)Y(I),(BZ(I,J),J=1,N)
ISN 0055           80 CONTINUE
ISN 0056              STOP
ISN 0057              END
```

BX COMPONENT

ALTITUDE =	90.	95.	100.	105.	110.	115.	120.	125.	130.	135.	140.	145.
Y= -1000.	0.	0.	0.	0.	0.	0.	0.	0.	0.	0.	0.	0.
Y= -900.	0.	0.	0.	0.	0.	0.	0.	0.	0.	0.	0.	0.
Y= -800.	0.	0.	0.	0.	0.	0.	0.	0.	0.	0.	0.	0.
Y= -700.	0.	0.	0.	0.	0.	0.	0.	0.	0.	0.	0.	0.
Y= -600.	0.	0.	0.	0.	0.	0.	0.	0.	0.	0.	0.	0.
Y= -500.	0.	0.	0.	0.	0.	0.	0.	0.	0.	0.	0.	0.
Y= -400.	0.	0.	0.	0.	0.	0.	0.	0.	0.	0.	0.	0.
Y= -300.	0.	0.	0.	0.	0.	0.	0.	0.	0.	0.	0.	0.
Y= -200.	0.	0.	0.	0.	0.	0.	0.	0.	0.	0.	0.	0.
Y= -100.	0.	0.	0.	0.	0.	0.	0.	0.	0.	0.	0.	0.
Y= 0.	0.	0.	0.	0.	0.	0.	0.	0.	0.	0.	0.	0.
Y= 100.	0.	0.	0.	0.	0.	0.	0.	0.	0.	0.	0.	0.
Y= 200.	0.	0.	0.	0.	0.	0.	0.	0.	0.	0.	0.	0.
Y= 300.	0.	0.	0.	0.	0.	0.	0.	0.	0.	0.	0.	0.
Y= 400.	0.	0.	0.	0.	0.	0.	0.	0.	0.	0.	0.	0.
Y= 500.	0.	0.	0.	0.	0.	0.	0.	0.	0.	0.	0.	0.
Y= 600.	0.	0.	0.	0.	0.	0.	0.	0.	0.	0.	0.	0.
Y= 700.	0.	0.	0.	0.	0.	0.	0.	0.	0.	0.	0.	0.
Y= 800.	0.	0.	0.	0.	0.	0.	0.	0.	0.	0.	0.	0.
Y= 900.	0.	0.	0.	0.	0.	0.	0.	0.	0.	0.	0.	0.
Y= 1000.	0.	0.	0.	0.	0.	0.	0.	0.	0.	0.	0.	0.

BY COMPONENT

ALTITUDE =	90.	95.	100.	105.	110.	115.	120.	125.	130.	135.	140.	145.
Y= -1000.	0.	0.	0.	0.	0.	0.	0.	0.	0.	0.	0.	0.
Y= -900.	0.	0.	0.	0.	0.	0.	0.	0.	0.	0.	0.	0.
Y= -800.	0.	0.	0.	0.	0.	0.	0.	0.	0.	0.	0.	0.
Y= -700.	0.	0.	0.	0.	0.	0.	0.	0.	0.	0.	0.	0.
Y= -600.	0.	0.	0.	0.	0.	0.	0.	0.	0.	0.	0.	0.
Y= -500.	0.	0.	0.	0.	0.	0.	0.	0.	0.	0.	0.	0.
Y= -400.	0.	0.	0.	0.	0.	0.	0.	0.	0.	0.	0.	0.
Y= -300.	0.	0.	0.	0.	0.	0.	0.	0.	0.	0.	0.	0.
Y= -200.	0.	0.	0.	0.	0.	0.	0.	0.	0.	0.	0.	0.
Y= -100.	0.	0.	0.	0.	0.	0.	0.	0.	0.	0.	0.	0.
Y= 0.	0.	0.	-126.	-346.	-440.	-440.	-440.	-440.	-440.	-440.	-440.	-440.
Y= 100.	0.	0.	-126.	-346.	-440.	-440.	-440.	-440.	-440.	-440.	-440.	-440.
Y= 200.	0.	0.	0.	0.	0.	0.	0.	0.	0.	0.	0.	0.
Y= 300.	0.	0.	0.	0.	0.	0.	0.	0.	0.	0.	0.	0.
Y= 400.	0.	0.	0.	0.	0.	0.	0.	0.	0.	0.	0.	0.
Y= 500.	0.	0.	0.	0.	0.	0.	0.	0.	0.	0.	0.	0.
Y= 600.	0.	0.	0.	0.	0.	0.	0.	0.	0.	0.	0.	0.
Y= 700.	0.	0.	0.	0.	0.	0.	0.	0.	0.	0.	0.	0.
Y= 800.	0.	0.	0.	0.	0.	0.	0.	0.	0.	0.	0.	0.
Y= 900.	0.	0.	0.	0.	0.	0.	0.	0.	0.	0.	0.	0.
Y= 1000.	0.	0.	0.	0.	0.	0.	0.	0.	0.	0.	0.	0.

BZ COMPONENT

ALTITUDE =	90.	95.	100.	105.	110.	115.	120.	125.	130.	135.	140.	145.
Y= -1000.	0.	0.	0.	0.	0.	0.	0.	0.	0.	0.	0.	0.
Y= -900.	0.	0.	0.	0.	0.	0.	0.	0.	0.	0.	0.	0.
Y= -800.	0.	0.	0.	0.	0.	0.	0.	0.	0.	0.	0.	0.
Y= -700.	0.	0.	0.	0.	0.	0.	0.	0.	0.	0.	0.	0.
Y= -600.	0.	0.	0.	0.	0.	0.	0.	0.	0.	0.	0.	0.
Y= -500.	0.	0.	0.	0.	0.	0.	0.	0.	0.	0.	0.	0.
Y= -400.	0.	0.	0.	0.	0.	0.	0.	0.	0.	0.	0.	0.
Y= -300.	0.	0.	0.	0.	0.	0.	0.	0.	0.	0.	0.	0.
Y= -200.	0.	0.	0.	0.	0.	0.	0.	0.	0.	0.	0.	0.
Y= -100.	0.	0.	2.	7.	17.	28.	39.	50.	61.	72.	83.	94.
Y= 0.	0.	0.	2.	7.	17.	28.	39.	50.	61.	72.	83.	94.
Y= 100.	0.	0.	-2.	-7.	-17.	-28.	-39.	-50.	-61.	-72.	-83.	-94.
Y= 200.	0.	0.	-2.	-7.	-17.	-28.	-39.	-50.	-61.	-72.	-83.	-94.
Y= 300.	0.	0.	0.	0.	0.	0.	0.	0.	0.	0.	0.	0.
Y= 400.	0.	0.	0.	0.	0.	0.	0.	0.	0.	0.	0.	0.
Y= 500.	0.	0.	0.	0.	0.	0.	0.	0.	0.	0.	0.	0.
Y= 600.	0.	0.	0.	0.	0.	0.	0.	0.	0.	0.	0.	0.
Y= 700.	0.	0.	0.	0.	0.	0.	0.	0.	0.	0.	0.	0.
Y= 800.	0.	0.	0.	0.	0.	0.	0.	0.	0.	0.	0.	0.
Y= 900.	0.	0.	0.	0.	0.	0.	0.	0.	0.	0.	0.	0.
Y= 1000.	0.	0.	0.	0.	0.	0.	0.	0.	0.	0.	0.	0.